Equilibrium Theory Analysis of Rectifying PSA for Heavy Component Production

Armin D. Ebner and James A. Ritter
Dept. of Chemical Engineering, Swearingen Engineering Center, University of South Carolina, Columbia, SC 29208

An isothermal equilibrium theory analysis, based on linear isotherms and a binary feed stream, was carried out to evaluate the feasibility of a rectifying PSA process for producing a pure heavy component at high recovery. Analytic expressions were derived to describe the performance of this process at the periodic state. The performance was also analyzed in terms of the different concentration and velocity profiles exhibited during various cycle steps that included the analysis of complex shock and simple wave interactions. Based on a parametric study, periodic behavior was established for a wide range of process conditions; and a design study with the PCB activated carbon$-H_2-CH_4$ system at 25°C further demonstrated the feasibility of a rectifying PSA cycle for producing a 100% CH_4 stream from a dilute feed stream ($y_{CH_4} = 0.01$) with a respectable recovery (80%), and reasonable process conditions. It also demonstrated the potential usefulness of an actual rectifying PSA process for bulk gas separation and purification.

Introduction

The easiest way to describe the essential features of a modern pressure swing adsorption (PSA) process, which can consist of multiple trains of columns processing a multicomponent feed, is to limit the discussion to a two-column system processing a binary feed mixture (Ruthven et al., 1994). A vast search of the patent literature revealed that nearly all PSA processes have been designed to produce a very pure light component at one end of the PSA unit and a mixture of the light and heavy components at the other end. This is accomplished mainly by using a small fraction of the light component product as purge. In essence, these kinds of PSA processes utilize a stripping reflux (purge) stream to remove the heavy component from the light product end of the column. There is no limitation on the purity of the light component; however, the enrichment of the heavy component is limited by the pressure ratio and rarely approaches it. A few PSA processes (Chue et al., 1995; Kikkinides et al., 1993; Kumar et al., 1992; Liu et al., 2000; Ruthven and Farooq, 1994; Sircar, 1990; Sircar and Hanley, 1993; Suh and Wankat, 1989; Yang and Doong, 1985) have been developed to produce two relatively high-purity products from a binary feed, but they necessarily require a high concentration of the heavy component in the feed, moderate to high pressure ratios, more complex cycle sequencing, or multiple trains of coupled PSA columns to achieve the separation. It is noteworthy that even in these special cases, the pressure-ratio constraint on the enrichment of the heavy component is not exceeded.

Hirose and coworkers (Diagne et al., 1994, 1995, 1996) and then, more recently, Ritter and coworkers (McIntyre et al., 2002a,b) developed and showed the potential of a two-bed PSA process that utilizes not only a stripping reflux stream at one end of the column, but also an enriching or rectifying reflux stream at the other end, with an intermediate feed position somewhere between the two ends. Hypothetically, this process has the potential to produce two pure products from a binary feed with the enrichment of the two components being constrained only by the mass balance. Diagne et al. (1994) also briefly mentioned that the rectifying section could be used alone to produce a pure heavy component at one end of the column and a mixture of the light and heavy components at the other end. This is accomplished mainly by using a large fraction of the heavy-component product as purge. In essence, this kind of PSA process utilizes an enriching reflux (purge) stream to remove the light component from the

Correspondence concerning this article should be addressed to J. A. Ritter.

heavy product end of the column. There is no limitation on the purity of the heavy component; however, the enrichment of the light component is once again limited by the pressure ratio. It is interesting, however, that the feasibility of a rectifying PSA process to produce a pure heavy component has never been demonstrated; it has only been explored for enriching trace components (Yoshida et al., 1998, 2000).

Therefore, the objective of this work is to analyze a simple twin-bed rectifying PSA process based on the isothermal, linear isotherm, equilibrium theory developed by Knaebel and Hill (1985) for a binary feed mixture. Analytic expressions for all of the important process performance indicators are derived and periodic operation is established. A design study is also carried out, which convincingly demonstrates the ability of a rectifying PSA process to produce a pure heavy component with high recovery from a binary feed stream containing mostly the light component.

Rectifying PSA Process Description

The rectifying PSA process is shown in Figure 1. This process consists of two columns operating in tandem and a four-step cycle. Each column undergoes the following four steps in sequence: (1) feed at constant low pressure (LHS bed Figure 1a), (2) pressurization (LHS bed in Figure 1b), (3) purge at constant high pressure (RHS bed Figure 1a), and (4) blowdown (RHS bed in Figure 1b). Two of the steps are carried out simultaneously at constant pressure (feed and purge, Figure 1a), and two of them are carried out simultaneously at varying pressure (pressurization and blowdown, Figure 1b). In this particular rectifying PSA cycle, products are withdrawn only during the feed and purge steps.

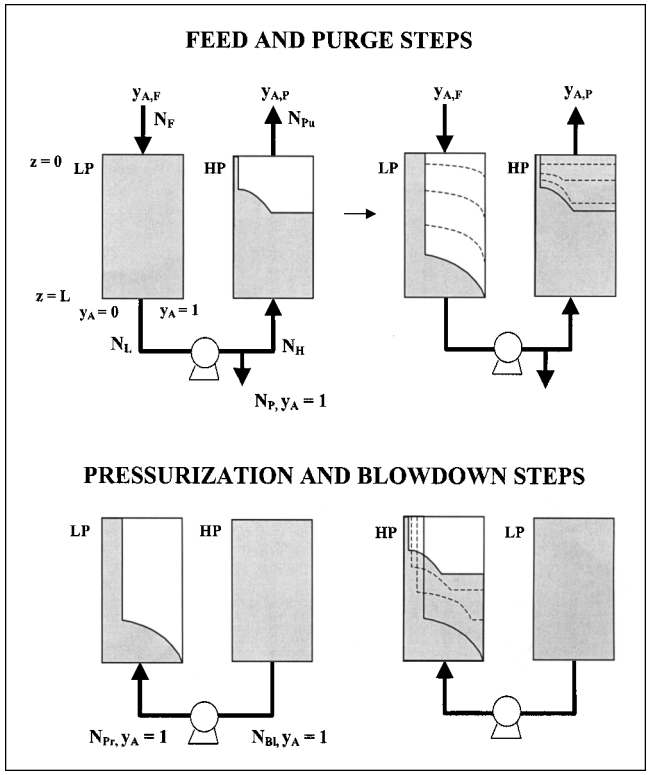

Figure 1. Operation of a rectifying PSA cycle.

Once the periodic state is reached and during the constant-pressure feed step, the feed (N_F) enters the top of the low-pressure bed (that is, LHS bed) while a completely enriched heavy product stream leaves the bottom. Some of this stream is taken as heavy (pure) product, but most is recycled to the high-pressure bed (that is, RHS bed) as purge. During this time, the high-pressure bed produces a light product depleted in the heavy component. At the beginning of the feed step, the low-pressure bed is completely saturated with the heavy component, but as the feed enters the top with a heavy-component mole fraction $y_{A,F}$, a downward-moving simple wave front develops. The feed step is stopped just prior to breakthrough of this front (that is, breakthrough of the light component into the heavy-component product stream). The valves at the tops of the beds are then closed and the pressure-changing steps begin. The LHS bed is pressurized from the bottom by pumping pure heavy component from the bottom of the RHS bed, which is initially saturated with heavy component at high-pressure and is now undergoing blowdown. A shock wave front moving upwards in the LHS bed starts to form, which depending upon the pressure ratio, either partially or fully develops. Due to pressurization, the gas-phase concentration upstream of this moving front, which is initially uniform and identical to $y_{A,F}$, decreases to $y_{A,P}$ and becomes the constant light-product effluent concentration during the next step. Once the pressures of the two beds are perfectly reversed, the valves at the tops of the beds are reopened, and the purge and feed steps begin in the LHS and RHS beds, respectively. Here, the purge recycle, which is pure heavy component, is taken from the product of the RHS bed, now undergoing the feed step, compressed, and fed into the bottom of the LHS bed. By the end of this step, the shock wave front is fully developed and located exactly at the top of the LHS bed, leaving this bed completely saturated with heavy component. Finally, the valves at the tops of the beds are again closed and the pressure-changing steps begin, where the effluent from the bottom of the LHS bed now undergoing blowdown is used to completely pressurize the RHS bed, and so on. Although this cycle has many similarities to a typical Skarstrom-type stripping PSA cycle, some very subtle differences exist, like feeding the low-pressure column while purging the high-pressure column and totally pressurizing one column with the blowdown gas from the other column.

Mathematical Model

Following the equilibrium theory analysis presented by Knaebel and Hill (1985), a single bed is assumed to operate isothermally, at pressures for which the gas behaves ideally and with no dissipative effects such as that due to diffusion or dispersion. The continuity equations for the heavy component A and total mass are, respectively, given by

$$\epsilon\left(\frac{\partial p_A}{\partial t}+\frac{\partial up_A}{\partial z}\right)+RT(1-\epsilon)\frac{\partial n_A}{\partial t}=0 \qquad (1)$$

$$\epsilon\left(\frac{\partial p}{\partial t}+\frac{\partial up}{\partial z}\right)+RT(1-\epsilon)\frac{\partial n}{\partial t}=0, \qquad (2)$$

with

$$p=p_A+p_B, \quad n=n_A+n_B, \qquad (3)$$

where u is the interstitial velocity, p is the absolute pressure, p_i is the partial pressure of species i, which is either A or B, ϵ is the interstitial volume, n_i is the moles of species i per unit volume of bed, T is the absolute temperature, and R is the universal gas constant. The linear isotherms are given by

$$n_i = \frac{k_i' p_i}{RT} = \frac{k_i' p y_i}{RT} \quad i = A \text{ or } B, \tag{4}$$

where k_i is the Henry's law constant of species i. By assuming no pressure drop in the bed (that is, $dp/dz = 0$), the interstitial velocity in the bed varies according to

$$u = \frac{-z}{\beta_B[1+(\beta-1)y_A]} \frac{1}{p} \frac{\partial p}{\partial t} \tag{5}$$

for the pressurization and blowdown steps when the bed is assumed closed (that is, $u = 0$) at $z = 0$; whereas, for the constant pressure, feed, and purge steps

$$\frac{u_1}{u_2} = \frac{[1+(\beta-1)y_{A,2}]}{[1+(\beta-1)y_{A,1}]} \tag{6}$$

are satisfied for any two locations 1 and 2 in the bed. The parameter β varies between $0 \le \beta \le 1$ and represents the degree of selectivity of the adsorbent toward the two species and is defined as

$$\beta = \frac{\beta_A}{\beta_B}, \tag{7}$$

where

$$\beta_i = \frac{1}{1+(1-\epsilon)k_i'/\epsilon}, \quad i = A \text{ or } B. \tag{8}$$

The concentration profiles are determined according to the method of characteristics. Diverging profiles (that is, corresponding to simple waves) are defined according to the following differential equations

$$\frac{dz}{dt} = \frac{\beta_A u}{1+(\beta-1)y_A} \tag{9}$$

$$\frac{dy}{dp} = \frac{(\beta-1)(1-y_A)y_A}{1+(\beta-1)y_A} \frac{1}{p}. \tag{10}$$

Solving these equations for the pressure-varying steps leads to the following characteristic equations that can be used to map the concentration profiles

$$\frac{y_A}{y_{Ao}} = \left(\frac{1-y_A}{1-y_{Ao}}\right)^{\beta} \pi^{(\beta-1)}, \quad \pi = p/p_o \tag{11}$$

$$\frac{z}{z_o} = \left(\frac{y_{Ao}}{y_A}\right)^{(\beta+1)/\beta} \frac{1+(\beta-1)y_A}{1+(\beta-1)y_{A,o}} \pi^{-1/\beta}. \tag{12}$$

The subscript o stands for any given point (z_o, P_o, y_o) of the characteristic. When the pressure is constant, the characteristics are defined with constant values of concentration (that is, $dy/dt = 0$ from Eq. 12), and thus from Eq. 11

$$z = z_o + \frac{\beta_A u}{1+(\beta-1)y_A}, \tag{13}$$

where u, according to Eq. 6, is also constant for every characteristic under constant-pressure conditions. Under converging profiles (that is, corresponding to shock waves) and assuming no mass accumulation at the shock wave, the velocity of the shock wavefront for varying pressures is given by

$$u_s = \left.\frac{dz}{dt}\right|_s = \frac{-\beta z}{[1+(\beta-1)y_{A,1}][1+(\beta-1)y_{A,2}]} \frac{1}{p} \frac{\partial p}{\partial t}, \tag{14}$$

and for constant pressures it is given by

$$u_s = \left.\frac{dz}{dt}\right|_s = \frac{\beta_A u_1}{1+(\beta-1)y_{A,2}} = \frac{\beta_A u_2}{1+(\beta-1)y_{A,1}}, \tag{15}$$

where the subscripts 1 and 2 denote the material immediately in front of and behind the shock wavefront.

The preceding developments are now combined with simple mass balances over each step to obtain the important process performance parameters. To obtain the purge-to-feed ratio, γ, which is defined here as the ratio between the velocity of the recycle gas entering the high-pressure bed to the velocity of the feed entering the low-pressure bed, an overall balance on all the mass entering and leaving the two-bed PSA unit while the four-step cycle is carried out. The calculation procedure entails a pursuit of the total mass of adsorbate that is present within a single bed at the end of each cycle step and assumes that the system has already reached the periodic state. Since the mass flows only from one bed to the other during the blowdown or pressurization steps, the total mass transferred is not evaluated and is defined simply as N_{Bl} or N_{pr}, respectively. The cycle starts with the feed step, with the bed at low pressure and saturated with the pure heavy component. It is relatively easy to show that for this situation the total mass of adsorbates, $M_{LP,o}$, in the bed is

$$M_{LP,o} = \frac{\epsilon A_{cs} L}{RT}\left(\frac{p_L}{\beta_A}\right) = \phi, \tag{16}$$

where for simplicity $M_{LP,o}$ is redefined as ϕ. Notice that during the feed step, the concentrations of the flows entering and leaving the bed (that is, $y_A = y_{A,F}$ and $y_A = 1$, respectively) remain constant (LHS bed in Figure 1a). As a consequence, the interstitial velocities remain constant at the boundaries and thus the total mass entering the bed during this step is

$$N_F = \int_0^{\Delta t} u_F \frac{p_L}{RT} \epsilon A_{cs}\, dt = u_F \frac{p_L}{RT} \epsilon A_{cs} \Delta t = \phi \Delta\tau, \tag{17}$$

and the total mass leaving the bed is

$$N_L = \phi\Delta\tau\frac{u_L}{u_F} = \phi\Delta\tau\frac{1+(\beta-1)y_{A,F}}{\beta}, \qquad (18)$$

where u_F and u_L are the interstitial velocities at the entrance and exit of the bed, respectively, and are related according to Eq. 6. The dimensionless time, τ, is defined as

$$\tau \equiv \frac{u_F}{L}\beta_A t. \qquad (19)$$

It is easy to show from Eqs. 9 and 6 that $\Delta\tau$ is related to the concentration of the feed according to

$$\Delta\tau \equiv \frac{u_F}{L}\beta_A\Delta t = \frac{\beta^2}{1+(\beta-1)y_{A,F}}. \qquad (20)$$

At the beginning of the purge step (RHS bed in Figure 1b), the total mass of adsorbates in the bed is equal to the total mass accumulated at the end of the feed step plus the mass that entered the bed during the pressurization step, that is,

$$M_{HP,o} = M_{LP,o} + N_F - N_L + N_{Pr}. \qquad (21)$$

Since the pressure of the bed is at p_H, the total mass entering the bed during this step is

$$N_H = \phi\Delta\tau\frac{u_H}{u_F}\frac{p_H}{p_L} = \phi\Delta\tau\frac{u_H}{u_F}\pi_T, \qquad (22)$$

whereas, the total mass leaving the bed is

$$N_{Pu} = \phi\Delta\tau\frac{u_P}{u_F}\frac{p_H}{p_L} = \phi\Delta\tau\frac{\beta}{1+(\beta-1)y_{A,P}}\frac{u_H}{u_F}\pi_T, \qquad (23)$$

where π_T is the pressure ratio (that is, $\pi_T = p_H/p_L$), and u_H and u_P are the interstitial velocities at the entrance and exit of the bed, respectively, for the purge step, which are related through Eq. 6. Notice also that during this step, the concentrations of the heavy component at the entrance and exit of the bed are constant and equal to 1 and y_{AP} (that is, the purge concentration), respectively. Finally, during the blowdown step, mass N_{Bl} leaves the bed, and at the end, the total mass in the bed returns to its initial total mass that was present at the beginning of the feed step, that is

$$M_{LP,o} = M_{LP,o} + N_F - N_L + N_{Pr} + N_H - N_{Pu} - N_{Bl}. \qquad (24)$$

It is easy to deduce from Eq. 5 that, at $z = L$ and for linear systems (that is, β_A and β_B constant), the mass that enters or leaves the bed during the pressure-varying steps depends only on the characteristics of the flow at the open end of the bed; hence, the mass leaving the bed during blowdown (N_{Bl}) is identical to the mass entering the bed during pressurization (N_{Pr}). After considering this fact and eliminating similar terms and replacing Eqs. 17, 18, 22 and 23 into Eq. 24, the purge-to-feed ratio becomes

$$\gamma = \frac{u_H}{u_F} = \frac{1-y_{A,F}}{1-y_{A,P}}\frac{1+(\beta-1)y_{A,P}}{\beta}\frac{1}{\pi_T}, \qquad (25)$$

where the concentrations of the feed and purge (that is, $y_{A,P}$ and $y_{A,F}$, respectively) are related through Eq. 11 with $\pi = \pi_T$. Four additional performance parameters are now defined. The ratio of the purge concentration to the feed concentration, defined here as the degree of depletion (D_D), is given by

$$D_D = \frac{y_{A,P}}{y_{A,F}} = \left(\frac{1-y_{A,P}}{1-y_{A,F}}\right)^{\beta}\pi_T^{(\beta-1)}, \quad \pi_T = p_H/p_L. \qquad (26)$$

The recycle ratio (R_R) is defined as the ratio between the moles of gas recycled into the high-pressure bed and the total moles of gas that leave the low-pressure bed, that is,

$$R_R = \frac{N_H}{N_L} = \frac{\beta}{1+(\beta-1)y_{A,F}}\pi_T\frac{u_H}{u_F} = \frac{1+(\beta-1)y_{A,P}}{1+(\beta-1)y_{A,F}}\frac{1-y_{A,F}}{1-y_{A,P}}. \qquad (27)$$

The extent of recovery (E_R) is simply the fraction of heavy component in the feed that is recovered as pure product, that is,

$$E_R = \frac{N_P}{y_{A,F}N_F} = \frac{N_L - N_H}{y_{A,F}N_F} = \frac{1}{y_{A,F}}\frac{y_{A,F}-y_{A,P}}{1-y_{A,P}}. \qquad (28)$$

Finally, the throughput (θ) is defined as the volumetric flow rate (at standard conditions, STP) of feed that is processed per unit mass of bed and is calculated from

$$\theta(\mathrm{STP}) = \frac{1}{2}\frac{\epsilon}{1-\epsilon}\frac{u_F}{(1+\chi)}\frac{1}{L\rho_s}\frac{p_L}{p_{\mathrm{STP}}}\frac{T_{\mathrm{STP}}}{T}, \qquad (29)$$

where χ is the ratio between the duration of the pressure-varying steps and that of the constant-pressure steps, that is,

$$\chi = \frac{\Delta t_p}{\Delta t}. \qquad (30)$$

Another variable that is important to the design of a rectifying PSA process is the maximum interstitial velocity that takes place during the four-step cycle. This variable is used later to determine the velocity of the feed. For a rectifying PSA unit, the maximum interstitial velocity during the constant-pressure steps occurs at the bottom of the bed (that is, at the most enriched zone in the low-pressure bed) during the feed step. Because the gas phase at this location contains only the heavy component, Eq. 6 gives the maximum interstitial velocity simply as

$$u_{\max,cp} = \frac{1+(\beta-1)y_{A,F}}{\beta}u_F. \qquad (31)$$

During the pressure-varying steps, the maximum interstitial velocity also occurs at the bottom of the bed where the gas is

flowing into or out of the bed and at the moment when the pressure in the bed is at a minimum, that is, at the end of the blowdown step or at the beginning of the pressurization step. From Eq. 5, the maximum interstitial velocity during the pressure-varying steps with the pressure varying linearly with time and identically in both columns is given by

$$u_{\max,pv} = \frac{L(\pi_T - 1)}{\beta_A \Delta t_p}. \tag{32}$$

Results and Discussion

Periodic and parametric behaviors

The first point that must be addressed concerns establishing periodic behavior in a rectifying PSA process. In other words, it must be shown that in all cases a shock wave of the fullest strength develops prior to the end of the purge step to ensure that the bed is completely saturated with the heavy product at the end of this step (as assumed in initiating the material balances around the cycle). The propagation of the concentration profiles, including the development of the shock wave, during the cycle was used to establish this periodic behavior. Figure 2 shows the moving fronts at different pressure levels during pressurization and different times during purge within the bed for $\beta = 0.5$, $y_{A,F} = 0.05$, and three different pressure ratios. The profiles were obtained by solving Eqs. 5 through 15 numerically for each of the cycle steps (Ebner et al., 2003), and the pressure ratios were selected to ensure that the shock wave that forms during the pressurization step becomes only partially developed ($\pi_T = 2.0$), just fully developed ($\pi_T = 3.82$), and past fully developed ($\pi_T = 6.0$) at the end of the pressurization step. The blowdown step was not included in this graph, as the bed always remains saturated with the heavy component during this step.

These results show very clearly that periodic behavior is easily established in a rectifying PSA cycle. Many other cases were also examined and in every one the shock wave is fully developed at the end of the purge step, thereby leaving the bed completely saturated with the heavy component. This is true even when the shock wave of the fullest strength formed during the purge step, as shown in Figure 2 for the case with $\pi_T = 2.0$. These results not only confirm that $\Delta\tau$ is independent of the pressure ratio, as Eq. 20 shows, but they also confirm that the external overall macroscopic mass balances that were used to derive the performance parameters completely agree with the differential mass balances that were used to obtain the various expressions that describe the moving simple and shock wavefronts that exist within the bed during a cycle (Ebner et al., 2003). Trends in the performance parameters can also be used to show the feasibility of a rectifying PSA process, especially R_R.

First note that four of the performance parameters, to wit, γ, D_D, R_R, and E_R depend only on β, $y_{A,F}$, and π_T (refer

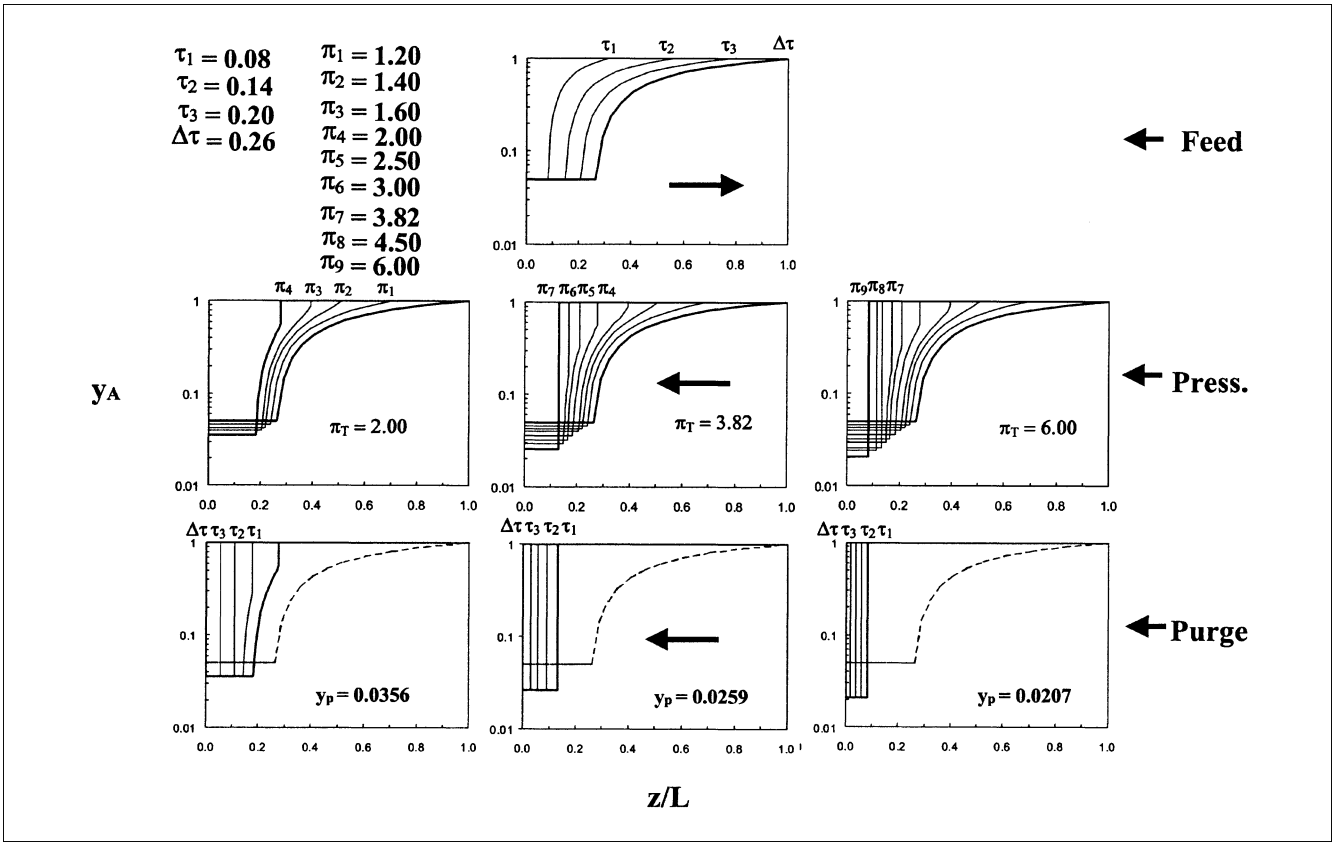

Figure 2. Bed concentration profiles during the feed, pressurization, and purge steps of a rectifying PSA cycle for three different pressure ratios with $y_{A,F} = 0.05$ and $\beta = 0.5$.

to Eqs. 25 through 28). Despite the fact that Eq. 20 must still be satisfied, this result is particularly remarkable, because it sets a thermodynamic limit that is independent of variables such as bed length, feed velocity, and cycle time. A graphical dependency of these performance parameters on β, $y_{A,F}$ and π_T is depicted in Figure 3 with $y_{A,F}$ fixed and β varying, and Figure 4 with β fixed and $y_{A,F}$ varying. The feasibility of a rectifying PSA process is clearly observed from all the R_R values being less than unity (Figures 3a and 4a). This means that the process contains enough gas to pressurize and purge the columns and still deliver a positive recovery of the pure heavy product. In other words, at the periodic state and for a range of practical process conditions, R_R is always less than unity, which indicates that a rectifying PSA process is entirely feasible.

Moreover, except for R_R in Figure 3a and γ in Figures 3b and 4b, the trends exhibited by the performance parameters are as expected and easily explained. For example, Figure 3c shows that when $y_{A,F}$ is fixed, E_R increases monotonically and asymptotically from 0 to around 0.9 at the extremes with increasing π_T and decreasing β for these particular conditions. A similar behavior is observed in Figure 3d with D_D, in that with increasing π_T and decreasing β, D_D varies from unity to a limiting value of around 0.1 at the extremes. Clearly, as the pressure ratio and the selectivity both increase, the process becomes more thermodynamically efficient, thereby making it easier to recover more of the heavy component, which in turn leaves less of it as a contaminant in the light-product stream. Figure 4 shows similar trends with fixed β, that is, R_R, E_R, and D_D all exhibit monotonic and asymp-

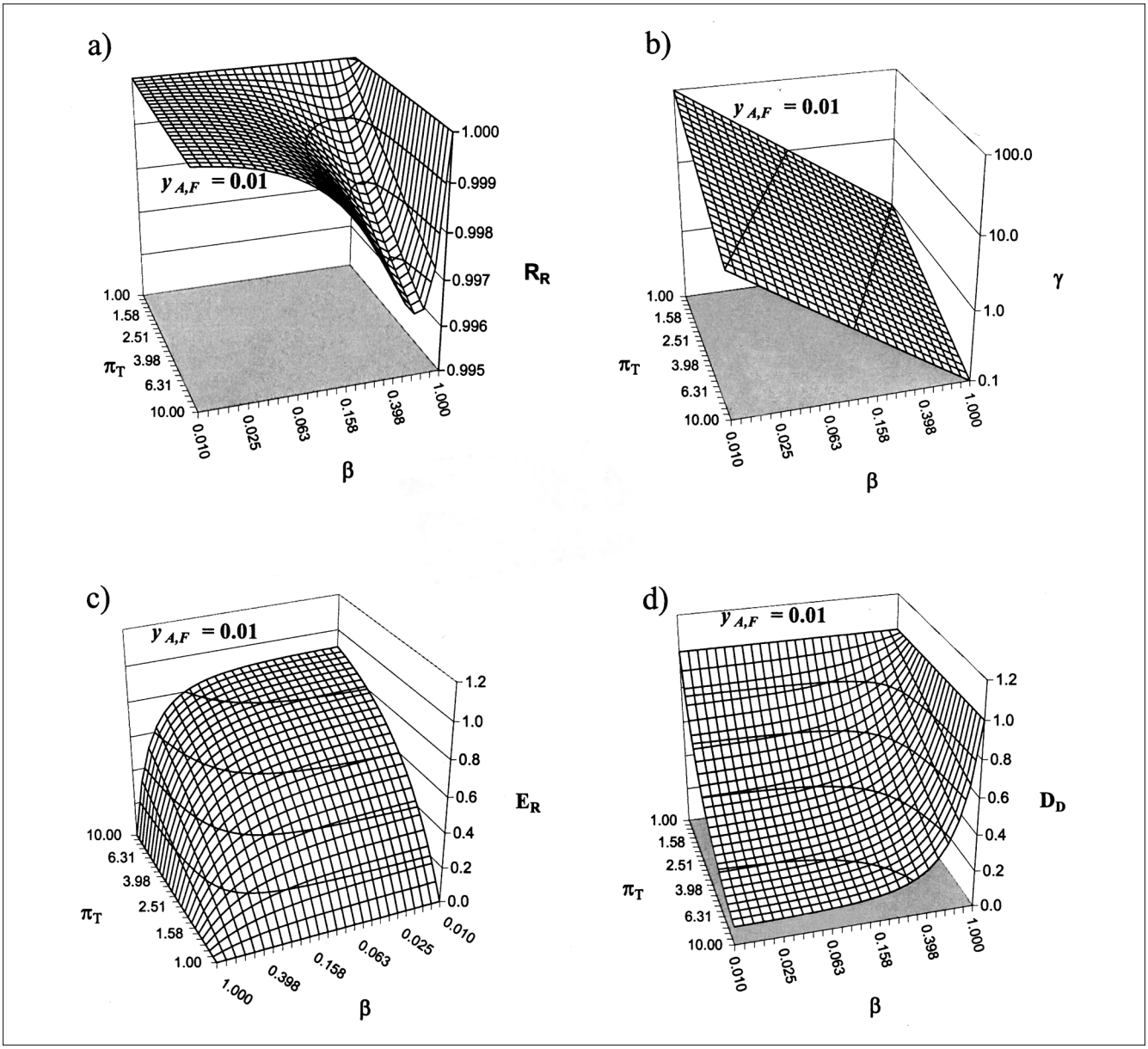

Figure 3. Effect of pressure ratio and selectivity on (a) recycle ratio, (b) purge-to-feed ratio, (c) extent of recovery, and (d) degree of depletion for $y_{A,F} = 0.01$.

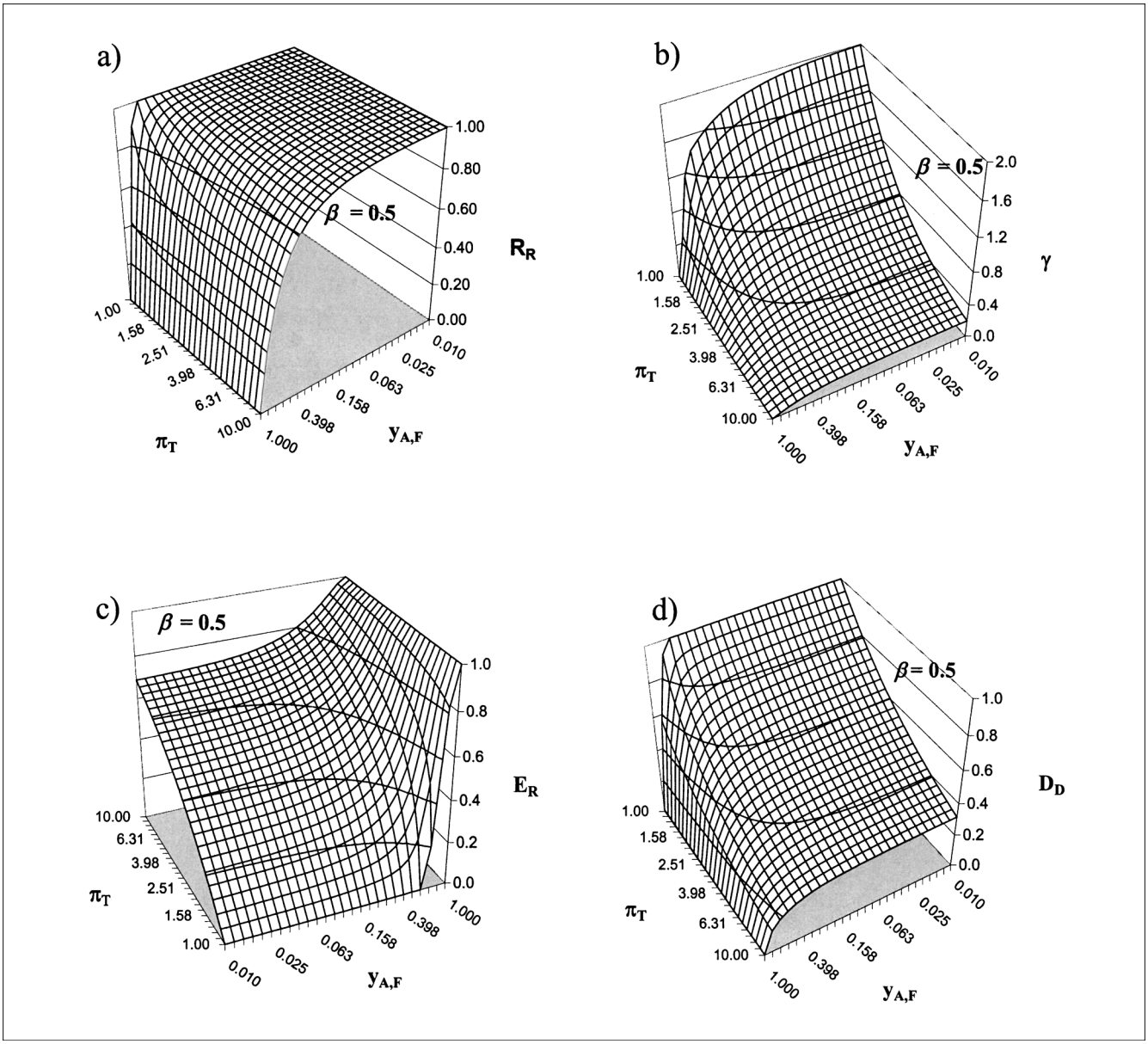

Figure 4. Effect of pressure ratio and heavy component feed concentration on (a) recycle ratio, (b) purge-to-feed ratio, (c) extent of recovery, and (d) degree of depletion for $\beta = 0.5$.

totic behavior. For example, Figure 4a shows that essentially for any π_T, R_R varies from zero to unity rather sharply as $y_{A,F}$ decreases from unity, indicating that most of the heavy-product gas must be recycled as high-pressure purge to achieve separation in a rectifying PSA cycle. Also E_R and D_D both increase with increasing π_T and $y_{A,F}$, as shown in Figures 4c and 4d, respectively. Clearly, the separation becomes exceedingly more difficult as the thermodynamics becomes less favorable; in other words, for a fixed β, as $y_{A,F}$ decreases, it takes a higher π_T to achieve the same E_R and D_D simply because it becomes increasingly more difficult to recover a pure heavy component from an increasingly more dilute feed stream.

In contrast to this monotonic behavior exhibited by most of the performance parameters, it is surprising that R_R exhibits a global minimum with respect to β in the proximity of $\beta = 0.6$ for a $y_{A,F} = 0.01$ (Figure 3a); similar results are realized for any other concentration. An explanation for this behavior becomes clear when using Eqs. 25, 27, and 31 to reexpress R_R in terms of the purge-to-feed ratio, pressure ratio, and maximum-velocity-to-feed-velocity ratio

$$R_R = \pi_T \frac{\gamma}{\left(\dfrac{u_{\max,cp}}{u_F}\right)}. \tag{33}$$

When β decreases, the adsorbent becomes more selective toward the heavy component, so that when the feed step begins, more heavy component desorbs and increases the gas-

phase flux toward the exit; this results in a larger γ, as is observed in Figure 3b. Because R_R is proportional to γ, the net effect of decreasing β is to increase R_R through γ. For identical reasons the maximum-velocity-to-feed-velocity ratio, in the denominator of Eq. 3, also increases. However, in this case, the R_R is forced to vary in the opposite direction, that is, to decrease. The result of these compromising trends is the existence of a minimum between the R_R and β: when β is small, the effect of γ is dominant and the first of the behaviors described earlier is observed, whereas when β is large or close to unity, the effect of the maximum-velocity-to-feed-velocity ratio is dominant and the second of the previously described behaviors is observed.

Another unusual and unexpected feature of this rectifying PSA cycle is its ability to establish periodic behavior with purge-to-feed ratios (γ) being less than or greater than unity, as shown in Figures 3b and 4b. This means that the high-pressure purge velocity can be higher or lower than the low-pressure feed velocity, and that a critical limiting value of γ does not seem to exist in a rectifying PSA process, as it does in some stripping PSA processes (Subramanian and Ritter, 1997). As stated earlier, when the selectivity of the adsorbent toward one of the species increases (that is, smaller β), the increase in the gas-phase flux caused by the heavy component desorbing during the feed step can be so strong that the recycled volumetric flow entering the high-pressure bed as purge can become larger than that of the feed, despite the compression influence of the larger pressure (that is, p_H). This explains why γ increases with decreasing β and $y_{A,F}$, as shown in Figure 3b with $y_{A,F}$ fixed and Figure 4b with β fixed, respectively. In contrast and similarly to a stripping PSA cycle, γ decreases with increasing π_T, as shown in both Figures 3b and 4b, because higher pressure ratios compensate for lower purge-to-feed ratios. Again, thermodynamics dictates the performance, wherein more purge gas is required at smaller pressure ratios, higher selectivities, or lower feed concentrations.

One final comment about Figures 3 and 4 concerns the constancy of these performance parameters with respect to $y_{A,F}$ in the low concentration region (that is, $y_{A,F} < 0.15$). In particular, D_D and E_R (Figures 3c and 4c, and Figures 3d and 4d, respectively) approach unitary, complementary limits, that is,

$$\lim_{y_{A,F} \to 0} D_D = \pi^{\beta - 1} \tag{34}$$

$$\lim_{y_{A,F} \to 0} E_R = 1 - \pi^{\beta - 1}, \tag{35}$$

where

$$\lim_{y_{A,F} \to 0} E_R + D_D = 1. \tag{36}$$

These inherent thermodynamic limits provide simple rules of thumb for these two variables when dealing with gas mixtures that are dilute in the heavy component.

Design study with the PCB activated carbon–H_2–CH_4 system

A brief design study with the PCB activated carbon–H_2–CH_4 system at 25°C (Ritter and Yang, 1987) is carried out to show that a rectifying PSA cycle is not only feasible, but also potentially useful for bulk phase separation and purification. To start, it is assumed that a rectifying PSA process is required to treat 5.0×10^{-4} m^3 (STP) s^{-1} of a gas mixture containing 1.0 vol. % CH_4 in a balance of H_2, with an extent of recovery of 80%. The concentration of the light-product stream, the performance parameters such as D_D, R_R, θ, and γ, the pressure ratio, and the bed dimensions are to be determined. The adsorbent physical properties, and other conditions and operating parameters for the process are summarized in Table 1. The duration of the constant-pressure steps is arbitrarily assumed to be 60 s. It is also desirable to restrict the maximum interstitial velocity during any part of the PSA cycle to be less than 1 m·s^{-1} and to use an aspect ratio (L/D) of 5 for the beds. The adsorption isotherms for this system are shown in Figure 5; the corresponding values of β_i for each component are given in Table 1. Clearly, CH_4 represents the heavy component (A) and H_2 represents the light component (B). The Henry's law regions for these components persist at most up to around 150 kPa ($\sim$1.5 atm); hence, p_H for this design study is fixed at 150 kPa.

Table 1. Process Parameters, and Adsorbent and Bed Properties Used in the Design Study*

$y_{A,F}$	0.01
V	5×10^{-4} m^3·s^{-1} (STP)
T	296 K
p_H	1.5×10^5 Pa
u_{max}	1 m·s^{-1}
Δt	60 s
L/D	5
ϵ	0.4
ρ_s	500 kg·m^3
k_A	1.048×10^{-8} kmol·kg^{-1}·Pa^{-1}
k_B	4.577×10^{-10} kmol·kg^{-1}·Pa^{-1}
β_A	0.0492
β_B	0.5420
β	0.0907

*$k_i' = P_s RT k_i$.

With $y_{A,F} = 0.01$, and from the definition of E_R (that is, Eq. 28), the concentration of the light-product stream be-

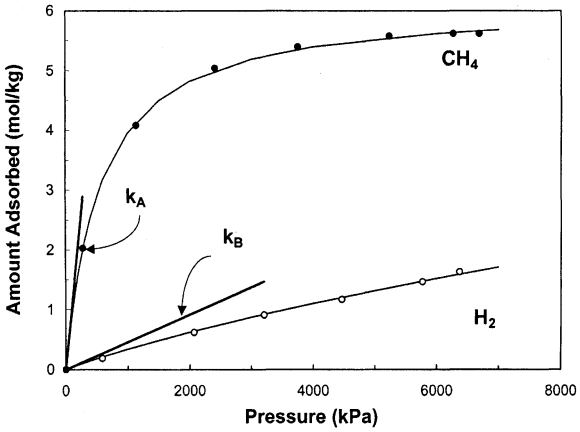

Figure 5. Adsorption isotherms for H_2 and CH_4 on PCB activated carbon at 25°C (Ritter and Yang, 1987).

comes

$$y_{A,P} = y_{A,F}\frac{1-E_R}{1-y_{A,F}E_R} = 0.00202, \tag{37}$$

and thus

$$D_D = \frac{y_{A,P}}{y_{A,F}} = 0.202. \tag{38}$$

Now, since $\beta = 0.0907$ for this system,

$$\pi_T = \frac{p_H}{p_L} = \left(\frac{y_{A,P}}{y_{A,F}}\right)^{1/(\beta-1)}\left(\frac{1-y_{A,F}}{1-y_{A,P}}\right)^{\beta/(\beta-1)} = 5.82 \tag{39}$$

and

$$R_R = \frac{1+(\beta-1)y_{A,P}}{1+(\beta-1)y_{A,F}}\frac{1-y_{A,F}}{1-y_{A,P}} = 0.9993, \tag{40}$$

using Eqs. 11 and 27, respectively. Consequently,

$$p_L = \frac{p_H}{\pi_T} = 25{,}760 \text{ Pa}, \tag{41}$$

and from Eqs. 25 and 20, respectively,

$$\gamma = \frac{u_H}{u_F} = \frac{1-y_{A,F}}{1-y_{A,P}}\frac{1+(\beta-1)y_{A,P}}{\beta}\frac{1}{\pi_T} = 1.875 \tag{42}$$

and

$$\Delta\tau = \frac{\beta^2}{1+(\beta-1)y_{A,F}} = 0.00830. \tag{43}$$

According to Eq. 19, the required interstitial velocity of the feed that ensures a 60-s duration for the constant pressure steps is governed by the following relationship

$$u_F = \frac{\Delta\tau L}{\Delta t\beta_A}, \tag{44}$$

where L is obtained from the specified aspect ratio of the column (that is, $L/D = 5$) and the known relationship between D and the volumetric flow, namely,

$$L = 5D = 5\left(\frac{4\dot{V}_F(\text{STP})}{\pi\epsilon u_F}\frac{p_{\text{STP}}}{p_L}\frac{T}{T_{\text{STP}}}\right)^{0.5}. \tag{45}$$

Combining Eqs. 44 and 45 and solving for u_F gives

$$u_F = \left(5\frac{\Delta\tau}{\Delta t\beta_A}\right)^{2/3}\left(\frac{4\dot{V}_F(\text{STP})}{\pi\epsilon}\frac{p_{\text{STP}}}{p_L}\frac{T}{T_{\text{STP}}}\right)^{1/3} = 1.10\times10^{-2} \text{ m·s}^{-1}, \tag{46}$$

which limits the maximum velocity of the feed step to be

$$u_{\max,cp} = \frac{1+(\beta-1)y_{A,F}}{\beta}u_F = 1.205\times10^{-1} \text{ m·s}^{-1}. \tag{47}$$

Note that this is well below the specified maximum velocity of 1 m·s^{-1}. The corresponding column diameter and length are

$$D = \left(\frac{4\dot{V}_F(\text{STP})}{\pi\epsilon u_F}\frac{p_{\text{STP}}}{p_L}\frac{T}{T_{\text{STP}}}\right)^{0.5} = 0.7804 \text{ m} \tag{48}$$

and

$$L = 5D = 3.92 \text{ m}. \tag{49}$$

Since it is desirable to carry out the pressurization step as fast as possible, the duration of the pressure-varying steps is obtained from Eq. 32, that is,

$$\Delta t_p = \frac{L(\pi_T - 1)}{\beta_A u_{\max,pv}} = 384.49 \text{ s} \tag{50}$$

with $u_{\max,pv} = 1$ m·s^{-1}. Hence, $\chi = 6.41$ and the throughput is

$$\theta(\text{STP}) = \frac{1}{2}\frac{\epsilon}{1-\epsilon}\frac{u_F}{(1+\chi)}\frac{1}{L\rho_s}\frac{p_L}{p_{\text{STP}}}\frac{T_{\text{STP}}}{T} = 5.94\times10^{-8}\frac{\text{m}^3\text{ (STP)}}{\text{kg·s}}. \tag{51}$$

The results from this design are summarized in Table 2, along with other designs carried out at (E_R) varying from 50%

Table 2. Performance Parameters and Column Design Variables for Different Extent of Recoveries*

E_R	0.50	0.70	0.80	0.90	0.95	0.98
$y_{A,p}$	0.0050	0.0030	0.0020	0.0010	0.0005	0.0002
D_D	0.5025	0.3021	0.2016	0.1009	0.0505	0.0202
R_R	0.9995	0.9994	0.9993	0.9992	0.9991	0.9991
π_T	2.1325	3.7324	5.8237	12.4687	26.7090	73.1409
p_L (Pa)	70341	40189	25757	12030	5616	2051
γ	5.1209	2.9253	1.8746	0.8755	0.4087	0.1492
$\Delta\tau$	0.0083	0.0083	0.0083	0.0083	0.0083	0.0083
u_F (m·s^{-1})	0.0079	0.0095	0.0110	0.0142	0.0183	0.0256
$u_{\max,cp}$ (m·s^{-1})	0.0862	0.1039	0.1205	0.1553	0.2002	0.2801
D (m)	0.5611	0.6762	0.7843	1.0109	1.3031	1.8231
L (m)	2.8056	3.3812	3.9217	5.0545	6.5156	9.1157
Δt_p (s)	64.5782	187.7750	384.4940	1,178.2182	3,404.6873	13,366.1591
χ	1.0763	3.1296	6.4082	19.6370	56.7448	222.7693
θ [m^3 (STP)·kg^{-1}·s^{-1}]	5.785×10^{-7}	1.662×10^{-7}	5.937×10^{-8}	9.954×10^{-9}	1.661×10^{-9}	1.565×10^{-10}

*Table 1 lists the fixed process parameters, and adsorbent and bed properties.

to 98%, while keeping all other conditions and parameters presented in Table 1 fixed. The separations achieved with this new rectifying PSA cycle are actually quite remarkable. For example, for the case with $E_R = 0.8$, a pure CH_4 stream can be produced with 80% recovery from a feed stream containing only 1.0 vol % CH_4. This can be achieved with two columns, each 3.92 m in length and 0.78 m in diameter utilizing a half-cycle time of about 445 s [$\Delta t\ (1+\chi)$] and a pressure ratio (π_T) of only 5.82. Note that only one pump is required, as it serves as both the compressor and vacuum pump. Moreover at a $D_D = 0.202$, the mole fraction of CH_4 in the light product stream is reduced considerably to a $y_{A,P} = 0.00202$ (that is, 2,020 ppm). It is instructive to view the concentration and velocity profiles corresponding to this rectifying PSA design to illustrate some of the unique features of this kind of cycle, especially during the pressure-changing steps.

Figure 6 shows the time evolution of the heavy-component concentrations and interstitial velocities in the bed for the feed, pressurization, and purge steps for this design ($E_R = 0.8$). Again, the blowdown step is not included here because the bed is saturated with the heavy component. The graphs are plotted in a log-log scale to help visualize the profiles because the main features occur in the last-fifth fraction of the bed. For identical reasons (with the exception of the initial and final conditions for the feed and purge steps, respectively), when the plots either coincide with the frame of the figures or are impossible to represent in a log-log scale, the initial and final conditions of each cycle step are plotted with thick and discontinuous lines, respectively. The letter L indicates the location of the lower end of the bed (that is, $L = 3.92$ m); and the numbers indicate different time and pressure events during the constant-pressure and pressure-varying steps, respectively, and are explained in the first two columns of Table 3. The direction of the flow is also indicated. The concentration profiles were obtained with the equations and analysis presented elsewhere (Ebner et al., 2003), and the velocity profiles were obtained from slightly modified forms of Eq. 6 for the feed and purge steps, that is,

$$u = \frac{[1+(\beta-1)y_{A,F}]}{[1+(\beta-1)y_A]}u_F \tag{52}$$

and

$$u = \frac{\beta}{[1+(\beta-1)y_A]}u_H = \frac{\beta}{[1+(\beta-1)y_A]}\gamma u_F, \tag{53}$$

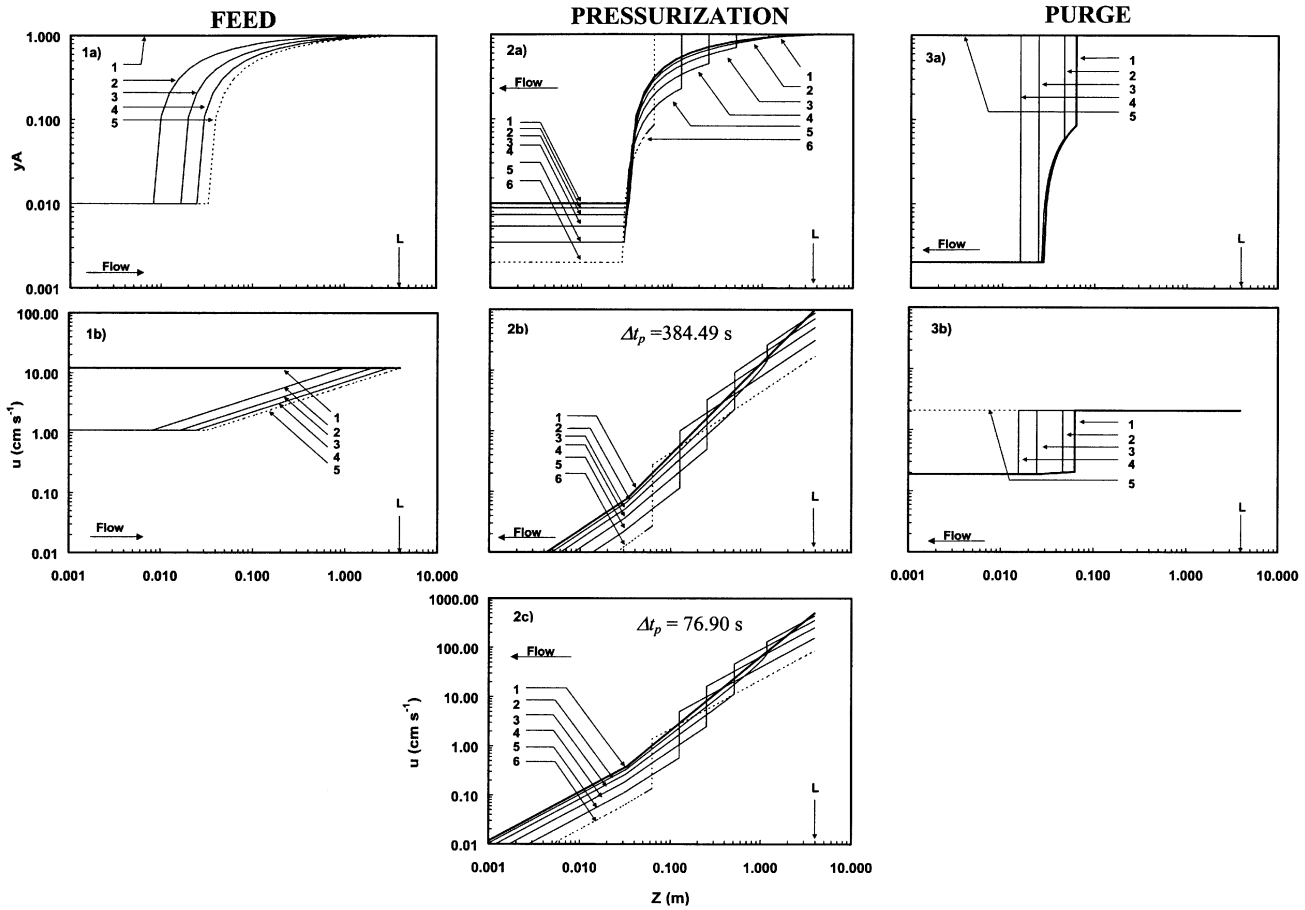

Figure 6. (a) Bed concentration and (b-c) interstitial velocity profiles during (1) feed, (2) pressurization, and (3) purge steps for the design conditions in Table 1 and design results in Table 2 with $E_R = 0.8$.

The pressures and times for each of the numbers assigned to the profiles are given in Table 3.

Table 3. Pressure and Times for Each Label in Figure 6, and Design Results for Two Different Constant-Pressure Step Durations (i.e., Δt)

Figure Label*	$\pi = p/p_L$	p (Pa)	τ	t (s)	τ	t (s)
Feed						
1	1.00	25,757	0.00000	0.0	0.00000	0.0
2	1.00	25,757	0.00208	15.0	0.00208	30.0
3	1.00	25,757	0.00415	30.0	0.00415	60.0
4	1.00	25,757	0.00623	45.0	0.00623	90.0
5	1.00	25,757	0.00830	60.0	0.00830	120.0
Pressurization						
1	1.00	25,757	0.00000	0.0	0.00000	0.0
2	1.13	29,233	0.00149	10.8	0.00094	13.6
3	1.40	36,168	0.00446	32.2	0.00281	40.6
4	1.97	50,686	0.01067	77.1	0.00672	97.2
5	3.20	82,381	0.02425	175.2	0.01527	220.8
6	5.82	150,000	0.05320	384.5	0.03351	484.4
Purge						
1	5.82	150,000	0.00000	0.0	0.00000	0.0
2	5.82	150,000	0.00207	15.0	0.00207	30.0
3	5.82	150,000	0.00500	36.2	0.00500	72.3
4	5.82	150,000	0.00623	45.0	0.00623	90.0
5	5.82	150,000	0.00830	60.0	0.00830	120.0
Design Parameters						
L (m)				3.922		4.941
u_F (m·s^{-1})				0.011		0.007
χ				6.408		4.037
Δt_p (s)				384.494		484.432

*As shown in Figure 6 for each cycle step.

respectively, and a slightly modified form of Eq. 5 for the pressurization step, that is,

$$u = \frac{-z}{\beta_B[1+(\beta-1)y_A]}\frac{1}{\pi}\frac{\pi_T-1}{\Delta t_p}. \tag{54}$$

The dimensionless time (that is, τ) for each pressure ratio listed under pressurization in Table 3 was obtained from Eq. 19 and the linear relationship between time and pressure for the pressure-varying steps, which in analogy to Eq. 32, is given by

$$\tau \equiv \frac{u_F\beta_A}{L}t = \frac{u_F\beta_A}{L}\frac{L(\pi-1)}{\beta_A u_{\max,p\upsilon}} = \frac{L(\pi_T-1)}{\beta_A u_{\max,p\upsilon}\Delta t}\frac{(\pi-1)}{(\pi_T-1)}$$
$$\times\frac{u_F\beta_A\Delta t}{L} = \chi\Delta\tau\frac{(\pi-1)}{(\pi_T-1)}. \tag{55}$$

It is remarkable that during the first 32.2 s of the pressurization step, which is less than one-tenth of the entire step duration, the shock wave advances through almost 80% of the column while significantly slowing down. This is a direct consequence of the shock wave passing through zones in the bed that are ever less saturated with the heavy component, which makes the shock wave slow down as adsorption occurs. Also, the velocities are continuously decreasing as a result of the upper end of the column being closed (see section 2b of Figure 6). Figure 6 also shows how a purge to feed ratio larger than unity ($\gamma = 1.875$) is manifest. Due to desorption of the heavy component during the feed step the velocities at the end of the bed are more than ten times higher than the feed velocity; note the steep velocity gradients in section 1b of Figure 6. These high velocities, although reduced by approximately the pressure ratio ($\pi_T = 5.82$, $R_R \approx 1$) when entering the bed during the purge step, are still γ times higher than the feed velocity, which again is due to the significant desorption that takes place during the feed step. Clearly, if the change in velocity during the feed step is less than that associated with the pressure change, then the corresponding γ would be less than unity.

It is worth insisting that the relative location of the concentration and velocity profiles are independent of the specified Δt. Table 3 shows, for example, the results for the same design, but with $\Delta t = 120$ s. In such a case, even though new values of L, u_F, and χ are obtained, the relative locations of the velocity and concentration profiles are identical to those shown in Figure 6 for the same numbered labels. Also, the duration of the pressure-varying steps, although fixed in this design study by the arbitrarily chosen maximum velocity of 1 m·s^{-1}, can be independently changed without affecting the results of the design. In other words, increasing or decreasing Δt_p only affects the velocities in the beds during the pressure-varying steps; it does not affect the position of the final concentration profile in section 1a of Figure 6 (No. 5) or the position of the initial concentration profile in section 3a of Figure 6 (No. 1). Nor does it affect any of the profiles in section 2a of Figure 6, as the pressure swing is dictated solely by the thermodynamic limits set by the high and low pressures. For example, for the same design with $E_R = 0.8$ and $\Delta t = 60$ s, section 2c of Figure 6 shows the velocity profiles during pressurization for $\chi = 1.282$ ($u_{\max,p\upsilon} = 5$ m·s^{-1}). A comparison of these profiles with those in section 2b of Figure 6 with $\chi = 6.41$ ($u_{\max,p\upsilon} = 1$ m·s^{-1}) reveals that the velocity gradients in section 2c of Figure 6 are much steeper for the shorter Δt_p, because the time available to progress from

the initial to the final concentration profiles shown in section 2a of Figure 6 decreases by a factor of 5 in this example. Of course, this would require a larger pump to handle the increased blowdown and pressurization rates and an adsorbent that can handle the specified maximum velocity.

Overall, it is noteworthy that all the trends observed in Tables 2 and 3 are intuitively consistent. For example, when the system is subjected to more demanding separation requirements (larger E_R values), the thermodynamics starts to play its role by demanding larger columns, larger pressure ratios, and larger cycle steps, to the point where θ is seriously affected. In this regard, the exceedingly long duration (almost 4 h) for the pressure-varying steps (that is, large χ) for the design with $E_R = 0.98$ is an interesting result. Although these steps are carried out at the specified maximum velocity of 1 $m \cdot s^{-1}$, a value that is approximately 36 times larger than the maximum velocity observed during the feed step (that is, 0.28 $m \cdot s^{-1}$), the large χ is simply a consequence of the enormous pressure ratio ($\pi_T = 73.14$) that is needed to achieve such a high E_R. Of course, as shown earlier, allowing for a larger maximum velocity in the design would decrease the value of χ considerably. Also, all the maximum interstitial velocities during the constant-pressure steps (that is, $u_{\max\ cp}$) for the broad range of conditions reviewed in Table 2 are far below the specified maximum velocity of 1 $m \cdot s^{-1}$, which strongly suggests that under reasonable time durations for the constant-pressure steps (that is, longer than a minute) the flows are expected to be low.

Conclusions

A model describing the behavior of a pressure-swing adsorption process designed for the rectification and purification of a heavy component from a binary gas mixture has been presented based on isothermal, linear isotherm, equilibrium theory. The resulting expressions were used to describe the performance of this process at the periodic state. More complex expressions (given elsewhere) requiring numerical solution were used to analyze the behavior of this process in terms of the evolution of the concentration and velocity profiles during the feed, purge, and pressurization steps. Interesting shock- and simple-wave interactions were revealed during the pressurization step and also during the purge step if the shock wave did not become fully developed during the pressurization step.

Periodic behavior was established for a wide range of process conditions, and the feasibility of this twin-bed rectifying PSA process was demonstrated based on a parametric study, and a design study with the PCB activated carbon–H_2–CH_4 system at 25°C. Typical design results with 80% CH_4 recovery showed that a pure CH_4 stream could be produced from a feed stream containing only 1.0 vol. % CH_4 in H_2. The column size, pressure ratio, and cycle time were also very reasonable.

It should be emphasized, however, that these very ideal equilibrium theory results represent the upper thermodynamic limit on the separation that can be achieved with a rectifying PSA process. In other words, in reality the separation will always be worse. Nevertheless, this analysis very convincingly showed that a rectifying PSA process is entirely feasible for producing a pure heavy component from a relatively dilute feed stream. In fact, under the right conditions, a rectifying PSA process has the potential to produce two relatively pure products from a binary feed stream, as shown in the design study. This analysis should also foster the development of other novel rectifying PSA cycles, and even combined rectifying–stripping PSA cycles, potentially mimicking the kinds of cycles so widely used in distillation processes.

Acknowledgments

The authors gratefully acknowledge financial support from the Westvaco Charleston Research Center and the Separations Research Program at the University of Texas at Austin.

Notation

A_{cs} = bed cross-sectional area, m^2
D = column diameter, m
D_D = degree of depletion defined in Eq. 26
E_R = extent of recovery defined in Eq. 28
k = Henry's law constant of species i, kmol kg^{-1} Pa^{-1}
k_i' = Henry's law constant of species i, m^3 gas phase m^{-3} adsorbent
L = column length, m
$M_{HP,o}$ = total mass of adsorbates at the beginning of the purge step, mol
$M_{LP,o}$ = total mass of adsorbates at the beginning of the feed step, mol
n_i = concentration of species i in the adsorbed phase, mol m^{-3} adsorbent
N_{Bl} = total mass of adsorbates leaving the bed during the blowdown step, mol
N_{Pr} = total mass of adsorbates entering the bed during the pressurization step, mol
N_F = total mass of adsorbates fed into the bed during the feed step, mol
N_L = total mass of adsorbates leaving the bed during the feed step, mol
N_H = total mass of adsorbates fed into the bed during the purge step, mol
N_P = total mass of adsorbates leaving the PSA unit during a half cycle, mol
N_{Pr} = total mass of adsorbates conveyed from one bed to the other during the pressure-varying steps, mol
N_{Pu} = total mass of adsorbates leaving the bed as light product during the purge step, mol
p = total pressure, $kg \cdot m^{-1} \cdot s^{-2}$
p_H = purge-step pressure, $kg \cdot m^{-1} \cdot s^{-2}$
p_L = feed-step pressure, $kg \cdot m^{-1} \cdot s^{-2}$
p_i = partial pressure of species i, $kg \cdot m^{-1} \cdot s^{-2}$
p_{STP} = atmospheric pressure, 101,350 $kg \cdot m^{-1} \cdot s^{-2}$
R = ideal gas constant, 8.314 $Pa \cdot m^3 \cdot K^{-1}$
R_R = recycle ratio defined in Eq. 27
t = time, s
T_{STP} = standard temperature, 273.15 K
T = bed temperature, K
u = interstitial velocity, $m \cdot s^{-1}$
u_H = interstitial velocity of the gas entering the bed during the purge step, $m \cdot s^{-1}$
u_F = interstitial velocity of the gas entering the bed during the feed step, $m \cdot s^{-1}$
u_L = interstitial velocity of the gas leaving the bed during the feed step, $m \cdot s^{-1}$
$u_{\max,cp}$ = maximum interstitial velocity during the constant-pressure steps, $m \cdot s^{-1}$
$u_{\max,pv}$ = maximum interstitial velocity during the pressure-varying steps, $m \cdot s^{-1}$
y_i = gas phase mol fraction of species i
$y_{i,P}$ = gas phase mol fraction of species i in the light product
$y_{i,F}$ = gas phase mol fraction of species i in the feed
z = distance from the top of the bed, m

Greek letters

β = selectivity of the adsorbent defined in Eq. 7
β_i = specific selectivity of species i defined in Eq. 8
χ = pressure-varying step duration to constant-pressure step duration ratio
ϵ = bed porosity, m^3 gas phase m^{-3} bed
γ = purge-to-feed ratio defined in Eq. 25
ϕ = total mass of adsorbate in the bed saturated with heavy component at the beginning of the feed step, mol
π = ratio of bed pressures at different times during a pressure-varying step
π_T = high-to-low-pressure ratio
θ = throughput defined in Eq. 29, m^3 feed gas kg^{-1} adsorbent s^{-1}
ρ_s = apparent adsorbent density, $kg \cdot m^{-3}$
τ = dimensionless time defined according to Eq. 19
$\Delta\tau$ = dimensionless time duration of a constant pressure step
Δt = time duration of a constant pressure step, s
Δt_p = time duration of a pressure-varying step, s

Subscripts and superscripts

A = heavy component
B = light component
o = state at the beginning of a pressure-varying step

Literature Cited

Chue, K. T., J. N. Kim, Y. J. Yoo, S. H. Cho, and R. T. Yang, "Comparison of Activated Carbon and Zeolite 13X for CO_2 Recovery from Flue Gas by Pressure Swing Adsorption," *Ind. Eng. Chem. Res.*, **34**, 591 (1995).

Diagne, D., M. Goto, and T. Hirose, "New PSA Process with Intermediate Feed Inlet Position and Operated with Dual Refluxes: Application to Carbon Dioxide Removal and Enrichment," *J. Chem. Eng. Jpn.*, **27**, 85 (1994).

Diagne, D., M. Goto, and T. Hirose, "Experimental-Study of Simultaneous Removal and Concentration of CO_2 by and Improved Pressure Swing Adsorption Process," *Energy Convers. Manage.*, **36**, 431 (1995).

Diagne, D., M. Goto, and T. Hirose, "Numerical Analysis of a Dual Refluxed PSA Process During Simultaneous Removal and Concentration of Carbon Dioxide Dilute Gas from Air," *J. Chem. Technol. Biotechnol.*, **65**, 29 (1996).

Ebner, A. E., K. D. Daniel, and J. A. Ritter, "Analysis of Simple and Shock Wave Interactions During a Rectifying PSA Cycle," *Adsorption*, in preparation (2003).

Kikkinides, E. S., R. T. Yang, and S. H. Cho, "Concentration and Recovery of CO_2 from Flue Gas by Pressure Swing Adsorption," *Ind. Eng. Chem. Res.*, **32**, 2714 (1993).

Knaebel, K. S., and F. B. Hill, "Pressure Swing Adsorption: Development of an Equilibrium Theory for Gas Separations," *Chem. Eng. Sci.*, **40**, 2351 (1985).

Kumar, R., W. C. Kratz, D. E. Guro, D. L. Rarig, and W. P. Schmidt, "Gas Mixture Fractionation to Produce Two High Purity Products by Pressure Swing Adsorption," *Sep. Sci. Technol.*, **27**, 509 (1992).

Liu, Y., J. A. Ritter, and B. K. Kaul, "Pressure Swing Adsorption Cycles for Improved Solvent Vapor Enrichment," *AIChE J.*, **46**, 540 (2000).

McIntyre, J. A., C. E. Holland, and J. A. Ritter, "High Enrichment and Recovery of Dilute Hydrocarbons by Dual Reflux Pressure Swing Adsorption," *Ind. Eng. Chem. Res.*, (2002a).

McIntyre, J. A., M. Yoshida, C. E. Holland, T. Hirose, and J. A. Ritter, "Stripping and Enriching Reflux Pressure Swing Absorption for High Enrichment and Recovery of Dilute Hydrocarbons," *Fund. of Adsorption 7*, K. Kaneko, H. Kanoh, and Y. Hanzawa, eds., IK International. Ltd., Chiba-City, Japan (2002b).

Ritter, J. A., and R. T. Yang, "Equilibrium Adsorption of Multicomponent Gas-Mixtures at Elevated Pressures," *Ind. Eng. Chem. Res.*, **26**, 1679 (1987).

Ruthven, D. M., and S. Farooq, "Concentration of a Trace Component by Pressure Swing Adsorption," *Chem. Eng. Sci.*, **49**, 51 (1994).

Ruthven, D., S. Farooq, and K. Knaebel, *Pressure Swing Adsorption*, VCH, New York (1994).

Sircar, S., "Production of Hydrogen and Ammonia Synthesis Gas by Pressure Swing Adsorption," *Sep. Sci. Technol.*, **25**, 1087 (1990).

Sircar, S., and B. F. Hanley, "Fractionated Vacuum Swing Adsorption Process for Air Separation," *Sep. Sci. Technol.*, **28**, 2553 (1993).

Subramanian, D., and J. A. Ritter, "Equilibrium Theory for Solvent Vapor Recovery by Pressure Swing Adsorption: Analytical Solution for Process Performance," *Chem. Eng. Sci.*, **52**, 3147 (1997).

Suh, S., and P. C. Wankat, "A New Pressure Swing Adsorption Process for High Enrichment and Recovery," *Chem. Eng. Sci.*, **44**, 567 (1989).

Yang, R. T., and S. J. Doong, "Gas Separation by Pressure Swing Adsorption: A Pore-Diffusion Model for Bulk Separation," *AIChE J.*, **31**, 1829 (1985).

Yoshida, M., A. Kodama, M. Goto, and T. Hirose, "Enrichment of Useful Trace Components in Air by New PSA Process," *Fundamentals of Adsorption 6*, F. Meunier, ed., Elsevier, New York (1998).

Yoshida, M., A. Kodama, M. Goto, T. Hirose, and J. A. Ritter, "Two Stage PSA for Enrichment of Trace Xenon From Atmospheric Air," *Adsorption Science and Technology*, D. D. Do, ed., World Scientific, River Edge, NJ (2000).

Manuscript received Oct. 23, 2001, and revision received Feb. 7, 2002.